Transactions of the TSME (2017) Vol. 5, No. 1, 55-64
Journal of Research and Applications in Mechanical Engineering

ISSN 2229-2152 print
DOI: 10.14456/jrame.2017.5

*Research Article*

# PERFORMANCE ENHANCEMENT IN A SOLAR AIR HEATER DUCT WITH INCLINED RIBS MOUNTED ON THE ABSORBER

**S. Skullong** *
*Energy Systems Research Group, Department of Mechanical Engineering, Faculty of Engineering at Sriracha, Kasetsart University Sriracha Campus, 199 M.6, Sukhumvit Rd., Sriracha, Chonburi 20230, Thailand*

**ABSTRACT:**
*The article deals with an experimental study on fluid friction and thermal characteristics in a solar air heater duct roughened artificially with inclined ribs. A new absorber plate with inclined-rib vortex generators is proposed in order to improve thermal performance for energy saving. The experimental work was carried out in the duct having a constant heat-flux on the absorber by varying airflow in the duct to let Reynolds number (Re) be 5300–23,000. Effects of two rib inclination angles ($\alpha$ = 45° and 60°) and three relative rib heights ($b/H=B_R$ = 0.1, 0.2 and 0.3) on flow friction and heat transfer behaviors are investigated. The experimental results reveal that the use of inclined rib vortex generators provides the considerable increase in heat transfer over the smooth-surface duct around 3.7–4.7 times while the friction factor (f) increases around 24.4–70.7 times. It is observed that the Nusselt number (Nu) increases with increasing the inclination angle and the relative height. The maximum thermal performance for using the rib vortex generators is about 1.4 at $\alpha$ = 45° and $B_R$ = 0.2.*

**Keywords:** *Solar air heater; Inclined rib; Heat transfer; Turbulent flow*

## 1. INTRODUCTION

Solar energy can be used endlessly and plays vital role in clean and sustainable energy sources. Solar air heater systems are widely used in heating that use solar energy. Improving thermal performance of the solar air heaters is crucial to meet energy costs and environment impact. The solar air heater applications are emphasized on drying, space heating and paint spraying operations. The solar air heater can be utilized effectively by enhancing heat transfer from the absorber to air. The most important thing in the design of solar air heaters is the surface shape of the absorber. In general, as air flow through a typical absorber plate (smooth plate), the heat transfer between the surface and airflow is typically low since the thermal boundary layer is developed. To increase the heat transfer rate the developed boundary layer must be disrupted by installing swirl/vortex-flow devices. Baffles/fins/ribs are the common types of such devices used to produce longitudinal vortex flows and to increase turbulence intensities resulting in the rise in heat transfer performance of the duct. Therefore, the application of fins/ribs is very rich and considered as the commonly used passive heat transfer enhancement [1] technique because fins/ribs placed repeatedly in the solar air heater duct lead to the interruption of the boundary layer and the recirculation flow induction.

In earlier studies, several researchers have proposed various artificial roughness geometries for augmenting the heat transfer. Han et al. [2] studied the influences of rib geometry including the attack angle and pitch-to-height ratio on thermal behaviors in a duct and suggested that the 45° ribs give higher thermal performance than the 90°

* Corresponding author: S. Skullong
E-mail address: sfengsps@src.ku.ac.th, sompol@eng.src.ku.ac.th

ribs. Han et al. [3] again proposed that the former two conditions lead to the rise in heat transfer with respect to the latter one. Chandra et al. [4] experimentally studied the flow friction and thermal characteristics in a square duct fitted with continuous ribs at $e/H$ = 0.0625 and $P/e$ = 8 on one, two, three and four walls of the duct. They reported that the heat transfer shows the increasing tendency with the increment in the number of ribbed walls, decreases with increasing Reynolds number while the friction factor gives the uptrend with both cases. Promvonge and Thianpong [5] carried out measurements on thermal behaviors for using wedge-ribs pointing upstream and downstream, triangular and rectangular ribs at $e/H$ = 0.3 and $P/e$ = 6.67 attached on the two opposite duct walls. They reported that the maximum heat transfer is seen at the in-line wedge rib pointing downstream while the staggered triangular rib provides the optimal thermal performance. An experimental investigation on the thermal behaviors of isosceles triangular ribs mounted on the two opposite walls of a channel was conducted by Thianpong et al. [6] who reported that the staggered ribs at $e/H$ = 0.1 and $P/H$ = 1.0 give the highest thermal performance. Prasad and Mullick [7] conducted an experiment to examine the influence of using small wire placed on the underside of the absorber as an artificial roughness. Sahu and Bhagoria [8] experimentally investigated flow resistance and thermal characteristics in a solar air heater with 90° transverse broken ribs. Skullong et al. [9] examined the rib size and arrangement effects on flow resistance and heat transfer behaviors in a solar air heater channel and indicated that the thin ribs placed on the absorber leads to higher heat transfer rate, friction loss and thermal performance than the square ribs.

Numerical investigations on turbulent flow and heat transfer characteristics in ducts/channels fitted with swirl/vortex-flow devices have been performed widely. Chaube et al. [10] investigated the heat transfer and turbulent flow behaviors using the SST $k$–$\omega$ turbulence model in a 2D-rib roughened (rectangular/chamfered rib) channel with heating one principal wall only. Tatsumi et al. [11] predicted numerically the flow friction and heat transfer in a square duct with discrete ribs attached obliquely and suggested that considerable heat transfer augmentation was at downstream of the rib due to stronger secondary flow. Eiamsa-ard and Promvonge [12] studied the two-dimensional heat transfer and flow resistance in a periodic groove channel. They reported that the use of grooved channel results in the increase in heat transfer around 158% higher than the smooth channel and the maximum thermal performance is up to 1.33 at $B/H$=0.75.

In the literature mentioned above, most studies are mainly emphasized on square or low aspect ratio ducts, rib pitch-spacings, arrangements and shapes. The investigation on the influence of rib angles and heights on thermal performance in solar air heaters has rarely been found. This is considered to be very helpful for improving the solar air heater system. The current article is concerned with an experimental study on the heat transfer in a solar air heater duct fitted with inclined ribs mounted on the absorber. The heat transfer and flow friction characteristics for two rib angles ($\alpha$) and various relative heights called the blockage ratio ($B_R$) are examined experimentally. The obtained results are presented for Reynolds number (Re) ranging from 5300 to 23,000.

## 2. EXPERIMENTAL SYSTEM

The schematic diagram of the experimental setup is shown in Fig. 1. It consisted of a test section, devices to measure the pressure, temperature and electrical power input, a high-pressure blower and a volumetric flow meter. The rectangular duct is connected to the suction side of a 1.5 kW high pressure blower. The air entered the solar air heater duct at a constant temperature (room temperature setting at 27 °C) and was measured by a volumetric flow meter. Thirty T-type thermocouples (1.5 mm diameter wire) were employed to measure the temperature distributions along the absorber surface while four RTD-type temperature sensors were applied to measure the air temperatures at the inlet and outlet. The accuracy of the thermocouples was within ±0.1°C. The pressure drop was measured from two static pressure taps located at the entry and the exit on the top channel wall using a digital differential pressure device. The uncertainty for the experimental heat balance was within ±5% and the maximum error of the airflow rate was within ±3%.

The test section depicted in Fig. 2 had the dimensions of 200 mm × 800 mm × 20 mm ($W \times L \times H$). A constant heat flux ($q''$= 600 W/m$^2$) was applied to the upper wall (or the absorber) while insulations were employed for the bottom and side walls. The inclined-ribbed upper plate was formed and accomplished by means of wire-EDM machining. The 5-mm thick aluminum inclined-ribs were mounted repeatedly on the absorber with a single axial pitch, $P$ = 60 mm (relative pitch, $P/H$=PR = 3). The ribs with three different relative heights ($b/H$=BR = 0.1, 0.2 and 0.3) and two inclination angles ($\alpha$ = 45° and 60°) are offered.

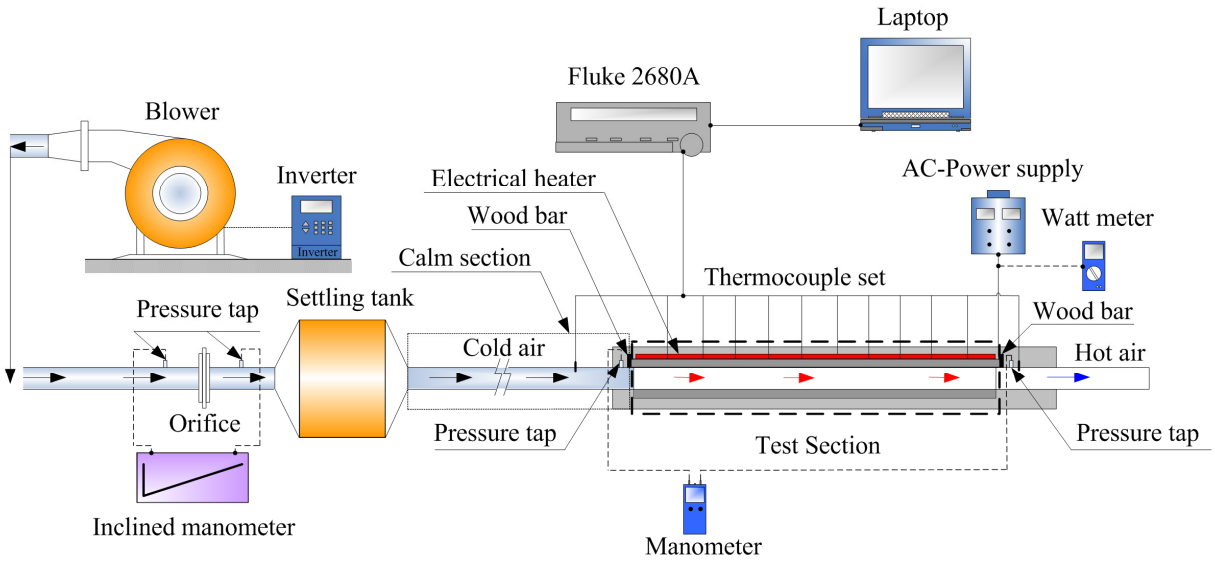


**Fig. 1.** Schematic sketch of experimental system.

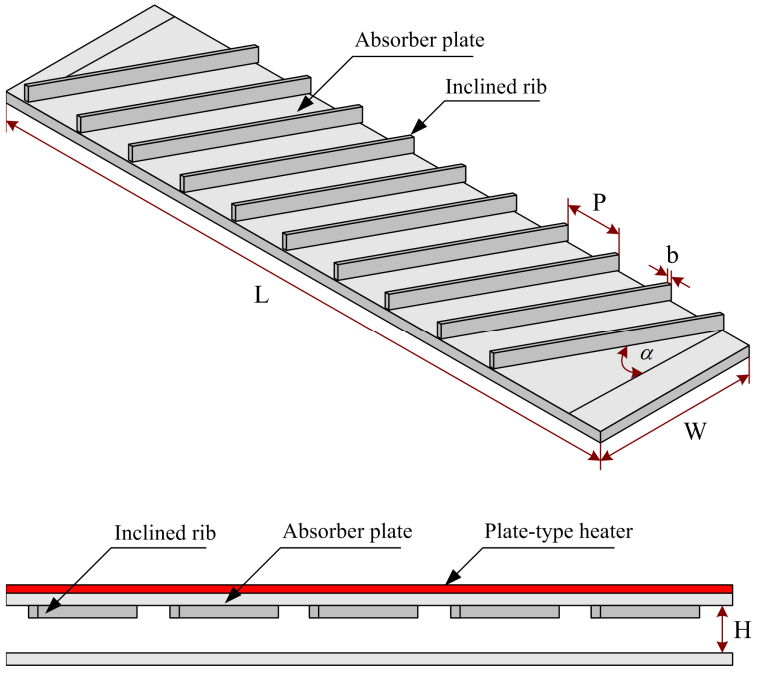


**Fig. 2.** Schematic of angle-ribbed absorber of solar air heater.

## 3. DATA PROCESSING

The data reduction for the heat transfer rate (Nusselt number, Nu), pressure drop (friction factor, *f*), flow condition (Reynolds number, Re) and thermal enhancement factor (at the same pumping power), are described in detail.

In the current experiment, air flows into the constant heat-fluxed test-duct. At a steady state condition, the rate of heat transfer is considered to be equal to the convection heat loss of the duct and expressed as:

$$Q_a = Q_{conv} \quad (1)$$

where

$$Q_{\mathrm{a}} = \dot{m} C_{\mathrm{p,a}} \left(T_{\mathrm{o}} - T_{\mathrm{i}}\right) \tag{2}$$

The convection heat transfer of the duct is calculated by

$$Q_{\mathrm{conv}} = hA\left(\tilde{T}_{\mathrm{w}} - T_{\mathrm{b}}\right) \tag{3}$$

in which

$$T_{\mathrm{b}} = (T_{\mathrm{o}} + T_{\mathrm{i}})/2 \tag{4}$$

and

$$\tilde{T}_{\mathrm{w}} = \sum T_{\mathrm{w}} /10 \tag{5}$$

where $T_w$ is the local wall temperature along the duct. The average wall temperature is evaluated from 10 points of the wall temperatures lined equally along the duct. The average heat transfer coefficient ($h$) and average Nusselt number (Nu) are written as

$$h = \dot{m} C_{\mathrm{p,a}} \left(T_{\mathrm{o}} - T_{\mathrm{i}}\right) / A\left(\tilde{T}_{\mathrm{w}} - T_{\mathrm{b}}\right) \tag{6}$$

The rate of heat transfer is obtained from knowing the Nu

$$\mathrm{Nu} = \frac{hD_{\mathrm{h}}}{k} \tag{7}$$

in which $D_{\mathrm{h}}$ is hydraulic diameter of the duct

$$D_{\mathrm{h}} = 4WH/(2W + 2H)$$

The $f$ computed by pressure loss across the test duct is written as

$$f = \frac{2}{\left(L/D_{\mathrm{h}}\right)} \frac{\Delta P}{\rho U^2} \tag{8}$$

in which $U$ is the mean air velocity in the duct.

The Re based on $D_{\mathrm{h}}$ is given by

$$\mathrm{Re} = UD_{\mathrm{h}}/\nu \tag{9}$$

All of thermo-physical properties of air are determined at overall bulk air temperature ($T_{\mathrm{b}}$) of Eq. (4).

The thermal enhancement factor (TEF) is given by

$$\mathrm{TEF} = \left(\frac{\mathrm{Nu}}{\mathrm{Nu}_0}\right)\left(\frac{f}{f_0}\right)^{-1/3} \tag{10}$$

where $h_0$ and $h$ are heat transfer coefficients for the smooth absorber and the ribbed-absorber ducts, respectively.

## 3. Results and Discussion

### *3.1 Verification of flat plate duct*

The comparison of the experimental heat transfer (Nu) and friction loss ($f$) results of the smooth/flat-plate duct in the present work and those from the standard equations [13] of Dittus-Boelter and Blasius, as given in Eqs. (11) and (12), is depicted in Fig. 3. In the figure, measured data are in good agreement with equations' data. The average deviation of the measured are within 7% for both Nu and $f$.

Dittus-Boelter equation:

$$\mathrm{Nu} = 0.023\mathrm{Re}^{0.8}\mathrm{Pr}^{0.4} \tag{11}$$

Blasius equation:

$$f = 0.316\,\mathrm{Re}^{-0.25} \tag{12}$$

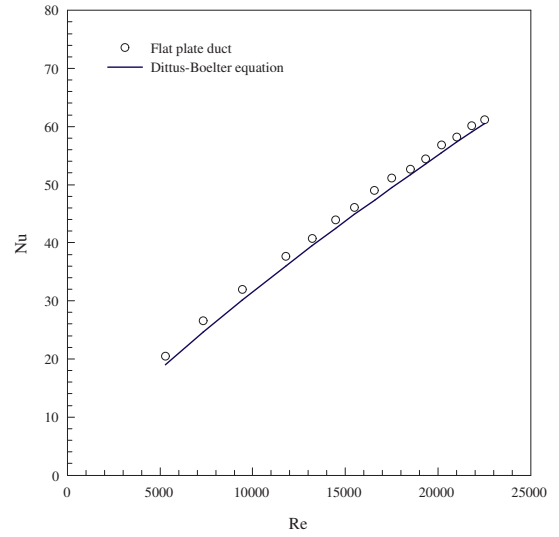


(a)

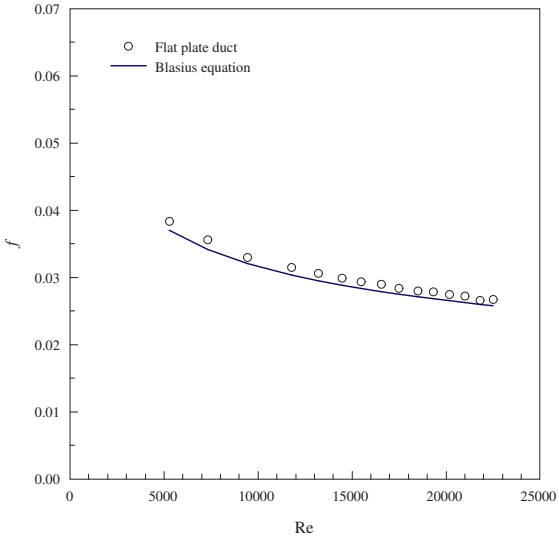


(b)

**Fig. 3.** Verification of (a) Nu and (b) *f* for flat-plate duct.

### *4.2 Heat transfer characteristics*

The heat transfer in the form of Nusselt Number (Nu) for the absorber incorporated with various inclination angles of ribs is analyzed and compared with the corresponding Nu values of the flat duct as shown in Fig 4(a). The solar air heater duct fitted with inclined ribs on the absorber shows higher heat transfer characteristics as compared to the flat duct. The Nu is found to increase with increasing $B_R$. Nu of the ribbed duct is seen to be higher than that of the flat duct around 73–78%, and the highest Nu is found at $\alpha = 60^o$ and $B_R = 0.5$. This is because the presence of the inclined rib induces stronger flow mixing resulting in destruction of the boundary layer and creates vortex-flows to prolong the residence time of flow.

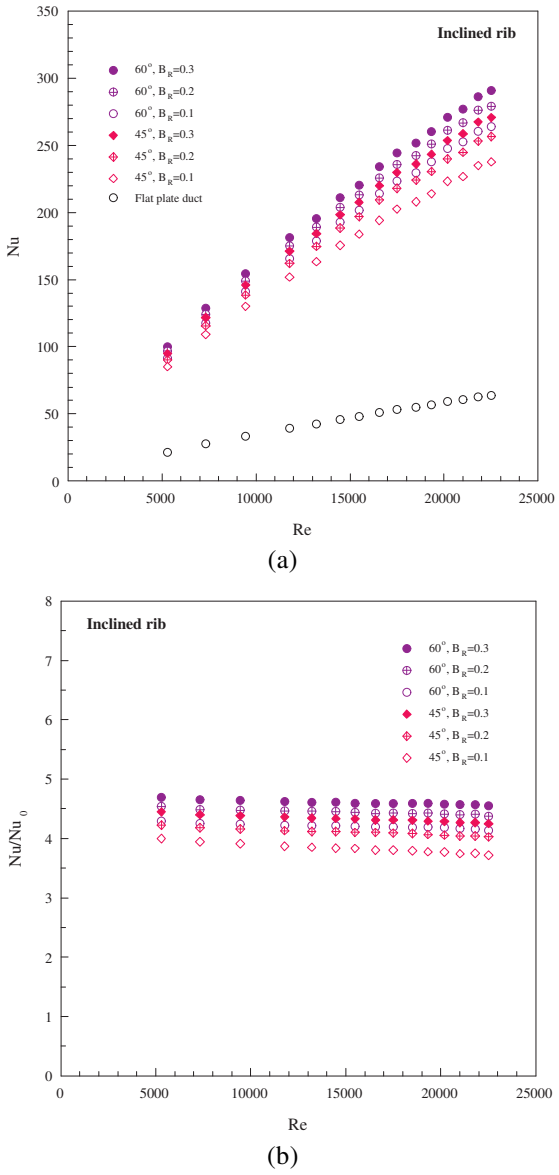


**Fig. 4.** Variations of (a) Nu and (b) $Nu/Nu_0$ with Re for inclined ribs.

The ratio of augmented Nu of artificial roughness (the ribbed absorber) to Nu of flat duct, ($Nu/Nu_0$) plotted against Re is depicted in Fig. 4(b). In the figure, $Nu/Nu_0$ tends to decrease slightly with the rise of Re for all cases. It is noted that the rib with $\alpha = 60^o$ and $B_R = 0.3$ provides the highest $Nu/Nu_0$. This is caused by the higher inclination angle of the rib at $B_R = 0.3$ that can more often interrupt the flow and can give stronger vortex flow strength leading to higher rate of heat transfer between the absorber surface and air. $Nu/Nu_0$ shows the slightly decreasing trend with the increase in Re. The quantitative results show that the mean $Nu/Nu_0$ values with $\alpha = 60^o$ and $45^o$ are about 4.2, 4.4 and 4.6; and 3.8, 4.1 and 4.3 times for $B_R$= 0.1, 0.2 and 0.3, respectively. The $Nu/Nu_0$ for the $60^o$ is higher than that for the $45^o$ ribs around 2–7%.

### *4.3 Friction characteristics*

The friction factor ($f$) for the ribbed absorber is analyzed and compared with the smooth/flat duct. Fig. 5(a) presents the effect of inclination angles ($\alpha$) and relative heights ($B_R$) of the rib vortex generators on $f$. As expected, the rib vortex generators can cause a significant pressure drop in comparison with the flat duct. The $f$ increases with the increase in the inclination angle and the relative height at the same Re. This is due to higher flow blockage

especially for using larger $B_R$ apart from the dissipation of dynamic pressure of the fluid due to larger surface area while the strength of longitudinal vortex is amplified as the inclination angle of ribs is increased, which leads to larger form drag. Compared with the flat duct at the Re range investigated, $f$ of the ribbed absorber is increased from 41–70.7% times for the $\alpha = 60^o$ case, and 24.4–44.1 times for the $\alpha = 45^o$ case.

Fig. 5(b) shows the variation of $f/f_0$ with Re for various $\alpha$ and $B_R$ values. In the figure, $f/f_0$ increases as a function of $\alpha$, $B_R$ and Re. The average $f/f_0$ values for the case of $\alpha = 60^o$ and $45^o$ are, respectively, about 48.8, 56.5 and 65.4; and 27.2, 32.3 and 41.5 for $B_R$ = 0.1, 0.2 and 0.3. The average $f/f_0$ for $\alpha = 60^o$ is about 40.9% higher than that for $\alpha = 45^o$.

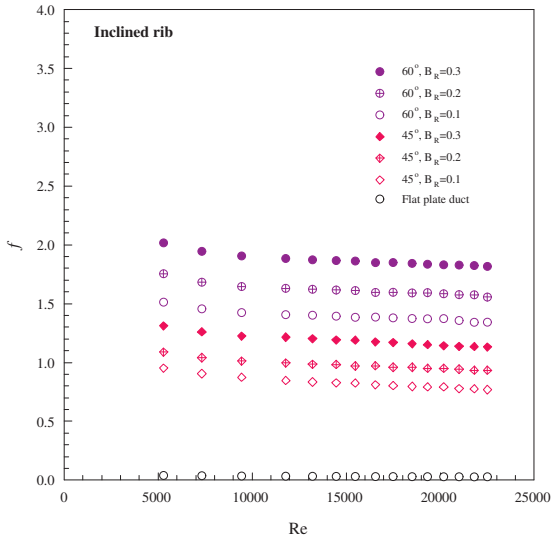


(a)

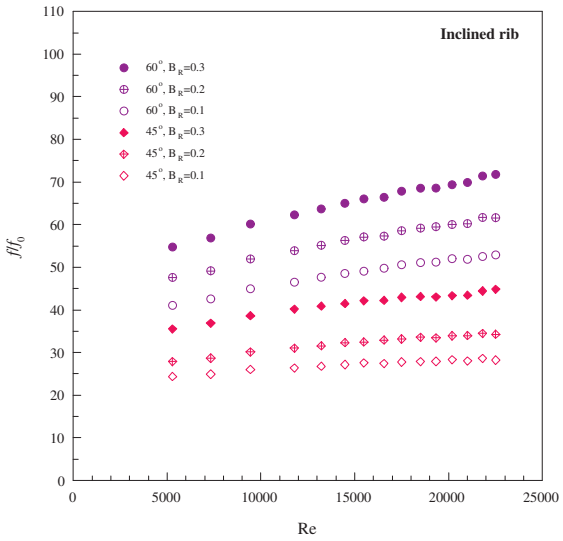


(b)

**Fig. 5.** Variations of (a) $f$ and (b) $f/f_0$ with Re for inclined ribs.

### *4.4 Thermal enhancement factor*

Figure 6 portrays the profile of thermal enhancement factor (TEF) with Re for the ribbed absorber with different $\alpha$ and $B_R$ values. This result is directly relevant to the trade-off between the enhanced Nu and the increased friction loss penalty. The highest TEF values from the $\alpha = 45^o$ ribbed absorber are, respectively, around 1.38, 1.4 and 1.35 at $B_R$= 0.1, 0.2 and 0.3. Also, the $\alpha = 45^o$ provides the highest TEF around 8–10% higher than the $\alpha = 60^o$. The

higher TEF of $\alpha = 45^{o}$ is attributed to its lower friction loss. Therefore, the best choice of this artificial roughness on the absorber is the rib with $\alpha = 45^{o}$ and $B_R = 0.2$ to achieve superior thermal performance.

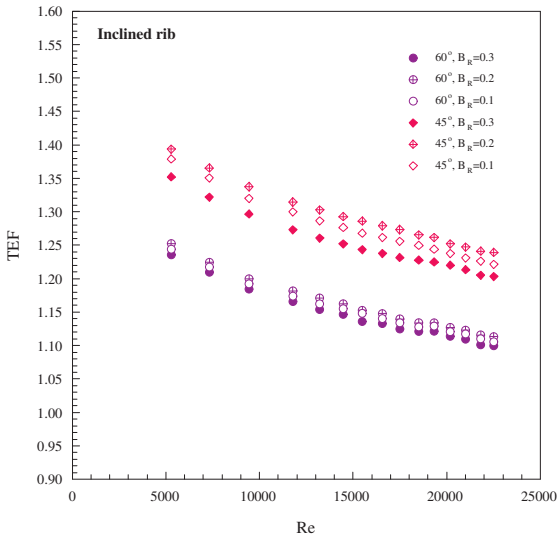


**Fig. 6.** Variation of TEF with Re for inclined ribs.

### *4.5 Comparison with other types of artificial roughness*

A comparison of TEF values of the present results for the ribbed absorber at $\alpha = 45^{o}$ and $B_R = 0.2$ with those of previous work such as square ribs (90°-rib) with three rib arrangements (one ribbed wall or single rib, in-line and staggered ribs on two opposite walls) of Skullong et al. [14] and transverse rib-groove [15] of Eiamsa-ard and Promvonge (TR and TG, PR=6.6) is displayed in Fig. 7. The TEF of the present work (ribbed absorber with $\alpha = 45^{o}$ and $B_R = 0.2$) is, in average, better than those of the artificial roughness mentioned earlier [14,15] around 13–26% higher depending on rib-types on the absorber.

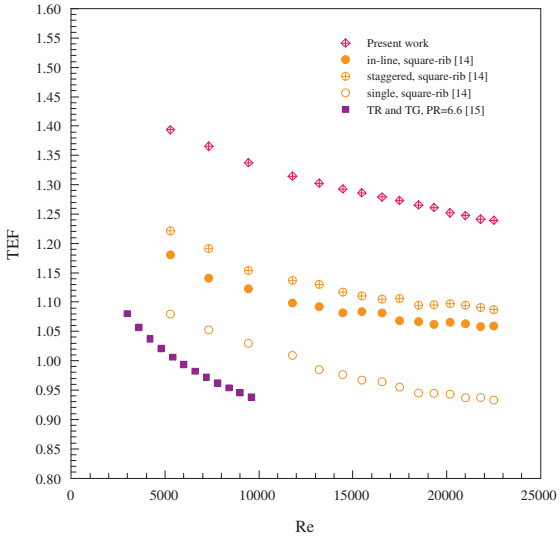


**Fig. 7.** TEF comparison between previous and present works.

## 5. CONCLUSIONS

Effects of artificial roughness on heat transfer and flow friction behaviors in a solar air heater duct having one principal wall roughened with inclined ribs have been experimentally examined. Two rib inclination angles ($\alpha$) and three relative roughness heights ($B_R$) are introduced in the current study. The major conclusions are:

- The rib parameters mentioned above yield a significant effect to the flow pattern in the solar air heater duct leading to the increment of both heat transfer and friction loss.
- As compared to the flat duct, the presence of the rib artificial roughness gives Nu up to 4.7 times while *f* rises up to 70.7 times in the range of parameters investigated. It is also observed that the maximum Nu and *f* for using the ribs are found at the largest $\alpha$ and $B_R$.
- At thermal performance comparison, the rib at $\alpha = 45^o$ and $B_R = 0.2$ provides the highest TEF of about 1.4 at Re=5300. Thus, the rib artificial roughness is a promising method for the performance improvement of a solar thermal system.

## NOMENCLATURE

| | |
|---|---|
| $A$ | absorber plate area ($m^2$) |
| $B_R$ | relative height of rib (=$b/H$) |
| $C_p$ | specific heat of air (J/kg K) |
| $D_h$ | hydraulic diameter of duct (m) |
| $f$ | friction factor of roughened duct |
| $f_0$ | friction factor of flat plate duct |
| $H$ | duct height (m) |
| $k$ | thermal conductivity of air (W/m K) |
| $\dot{m}$ | mass flow rate of air (kg/s) |
| $L$ | length of test section |
| Nu | Nusselt number of roughened duct |
| $Nu_0$ | Nusselt number of flat duct |
| $P$ | pitch between rib (m) |
| $Q$ | heat transfer rate (W) |
| Pr | Prandtl number |
| $P_R$ | relative longitudinal pitch (=$P/H$) |
| Re | Reynolds number |
| $T_i$ | inlet air temperature ($^o$C) |
| $T_o$ | outlet air temperature ($^o$C) |
| $T_b$ | bulk mean air temperature ($^o$C) |
| TEF | thermal enhancement factor |
| $W$ | duct width (m) |

*Greek symbols*

| | |
|---|---|
| $\mu$ | dynamic viscosity (kg/m s) |
| $\alpha$ | inclination angle (degree) |

*Subscripts*

| | |
|---|---|
| a | air |
| w | wall |

## REFERENCES


[1] Liu, S., and Sakr, M. A comprehensive review on passive heat transfer enhancements in pipe exchangers, Renew. Sustain. Energy Rev., Vol. 19, 2013, pp. 64-81.

[2] Han, J.C., Glicksman, L.R. and Rohsenow, W.M. An investigation of heat transfer and friction for rib-roughened surfaces, Int. J. Heat Mass Transf., Vol. 21, 1978, pp. 1143-1156.

[3] Han, J.C., Zhang, Y.M. and Lee, C.P. Influence of surface heat flux ratio on heat transfer augmentation in square channels with parallel, crossed, and V-shaped angled ribs, ASME J. Turbomach, Vol. 114, 1992, pp. 872-880.

[4] Chandra, P.R., Alexander, C.R. and Han, J.C. Heat transfer and friction behaviour in rectangular channels with varying number of ribbed walls, Int. J. Heat Mass Transf., Vol. 46, 2003, pp. 481-495.
[5] Promvonge, P. and Thianpong, C. Thermal performance assessment of turbulent channel flow over different shape ribs, Int. Commun. Heat Mass Transf., Vol. 35(10), 2008, pp. 1327-1334.
[6] Thianpong, C., Chompookham, T., Skullong, S. and Promvonge, P. Thermal characterization of turbulent flow in a channel with isosceles triangular ribs, Int. Commun. Heat Mass Transf., Vol. 36(7), 2009, pp. 712-717.
[7] Prasad, K. and Mullick, S.C. Heat transfer characteristics of a solar air heater used for drying purposes, Appl. Energy, Vol. 13(2), 1983, pp. 83-93.
[8] Sahu, M.M.and Bhagoria, J.L. Augmentation of heat transfer coefficient by using 90o broken transverse ribs on absorber plate of solar air heater, Renew. Energy, Vol. 30, 2005, pp. 2063-2075.
[9] Skullong, S., Thianpong, C. and Promvonge, P. Effects of rib size and arrangement on forced convective heat transfer in a solar air heater channel, Heat Mass Transf., Vol. 51, 2015, pp. 1475-1485.
[10] Chaube, A., Sahoo, P.K. and Solanki, S.C. Analysis of heat transfer augmentation and flow characteristics due to rib roughness over absorber plate of a solar air heater, Renew. Energy, Vol. 31, 2006, pp. 317-331.
[11] Tatsumi, K., Iwai, H., Inaoka, K. and Suzuki, K. Numerical analysis for heat transfer characteristics of an oblique discrete rib mounted in a square duct, Numerical Heat Transfer, Part A: Applications, Vol. 44(8), 2003, pp. 811-831.
[12] Eiamsa-ard, S. and Promvonge, P. Numerical study on heat transfer of turbulent channel flow over periodic grooves, Int. Commun. Heat Mass Transf., Vol. 35, 2008, pp. 844-852.
[13] Incropera, F. and Dewitt, P.D. Fundamentals of heat and mass transfer, 6th edition, 2007, Wiley, USA.
[14] Skullong, S., Thianpong, C. and Promvonge, P. Effects of rib size and arrangement on forced convective heat transfer in a solar air heater channel, Int. Commun. Heat Mass Transf., Vol. 51, 2015, pp. 1475-1485.
[15] Eiamsa-ard, S. and Promvonge, P. Thermal characteristics of turbulent rib-grooved channel flows, Int. Commun. Heat Mass Transf., Vol. 36, 2009, pp. 705-711.